

Supporting Information

Ring-Opening Polymerization of Cyclic Esters by Phenoxy-Thioether Complexes Derived from Biocompatible Metals

Alessia Pilone, Marina Lamberti,* Mina Mazzeo,* Stefano Milione, Claudio Pellecchia.

*Department of Chemistry and Biology, University of Salerno. I-84084, via Ponte don Melillo,
Fisciano, Salerno, Italy.*

Table of contents

Figure S1. ^1H NMR of complex 1	S2
Figure S2. ^1H NMR of complex 2	S2
Figure S3. ^1H NMR of complex 3	S3
Figure S4. ^1H NMR of complex 4	S3
Figure S5. ^1H NMR of complex 5	S4
Figure S6. ^1H NMR of complex 6	S4
Figure S7. Eyring plot for the temperature-dependent fluxional process for complex 2	S5
Figure S8. Variable-temperature ^1H NMR spectra of 3 in toluene- d_8	S6
Figure S9. Eyring plot for the temperature-dependent fluxional process for complex 3	S6
Figure S10. Variable-temperature ^1H NMR spectra of homoleptic complex 6 in CD_2Cl_2	S7
Figure S11. ^1H NMR spectrum (400 MHz, CDCl_3 , 298 K) of oligomers of L-LA	S7
Figure S12. Plausible mechanism for the polymerization of L-LA by 3 in the absence of alcohol..	S8
Figure S13. ^1H NMR spectrum (400 MHz, CDCl_3 , 298 K) of the CL-LA block copolymer	S8
Figure S14. Pseudofirst-order kinetic plot for ROP of L-LA promoted by 3	S9
Figure S15. Semilogarithmic plot of LA conversion with time for 3 at 323 K.....	S9
Figure S16. Enlargement of the linear part of graphic in figure S14.....	S10

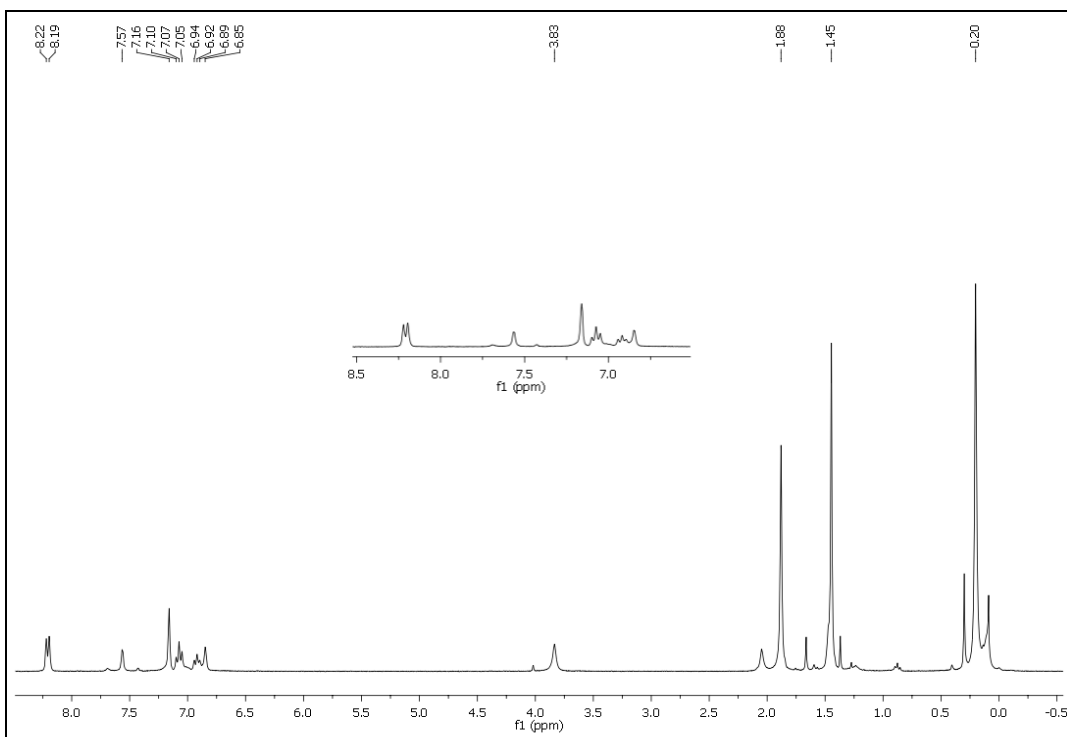


Figure S1. ¹H NMR of complex 1 (300 MHz, C₆D₆, 298 K).

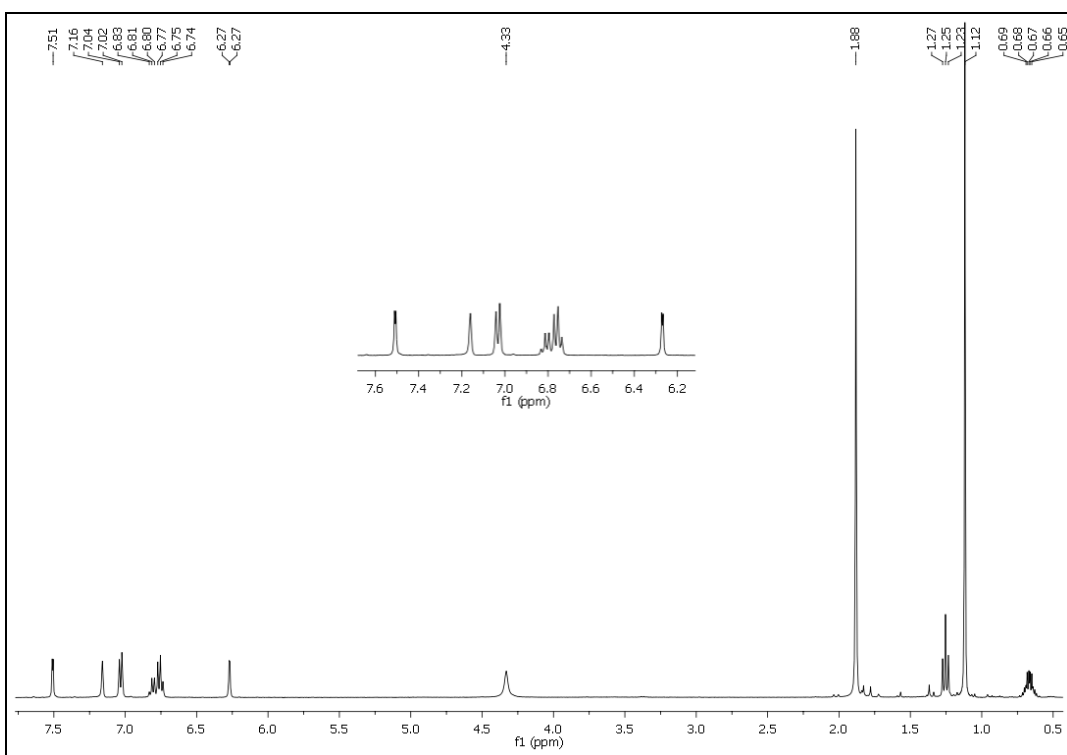


Figure S2. ¹H NMR of complex 2 (400 MHz, C₆D₆, 298 K).

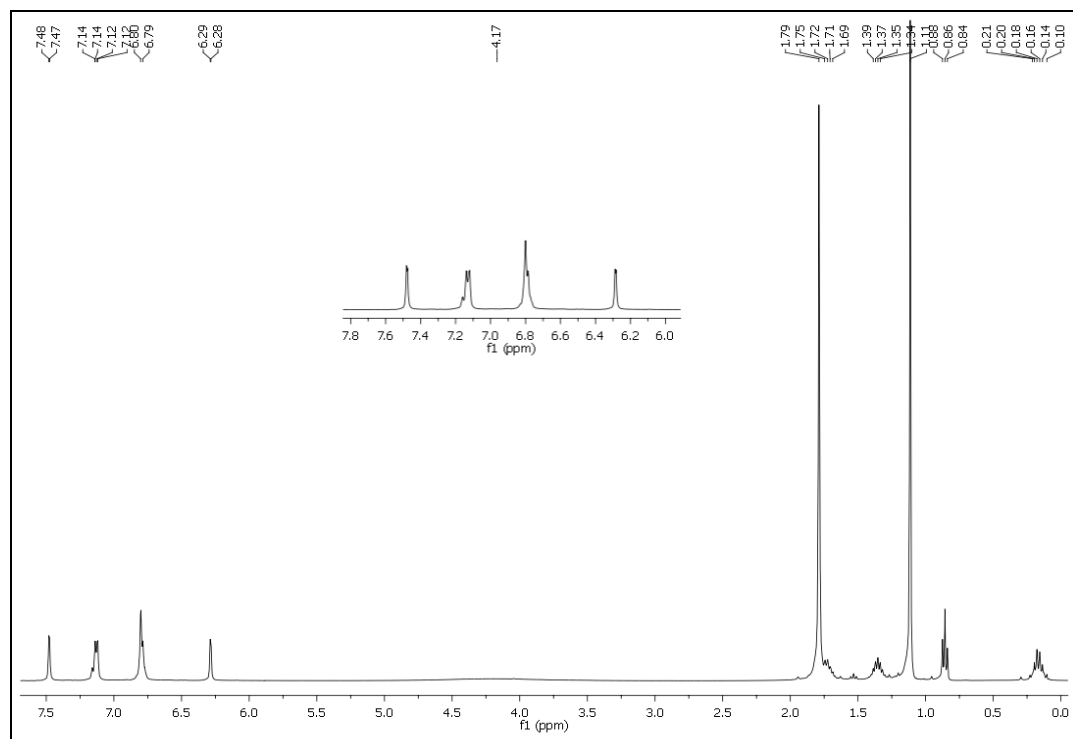


Figure S3.¹H NMR of complex **3** (400 MHz, C₆D₆, 298 K).

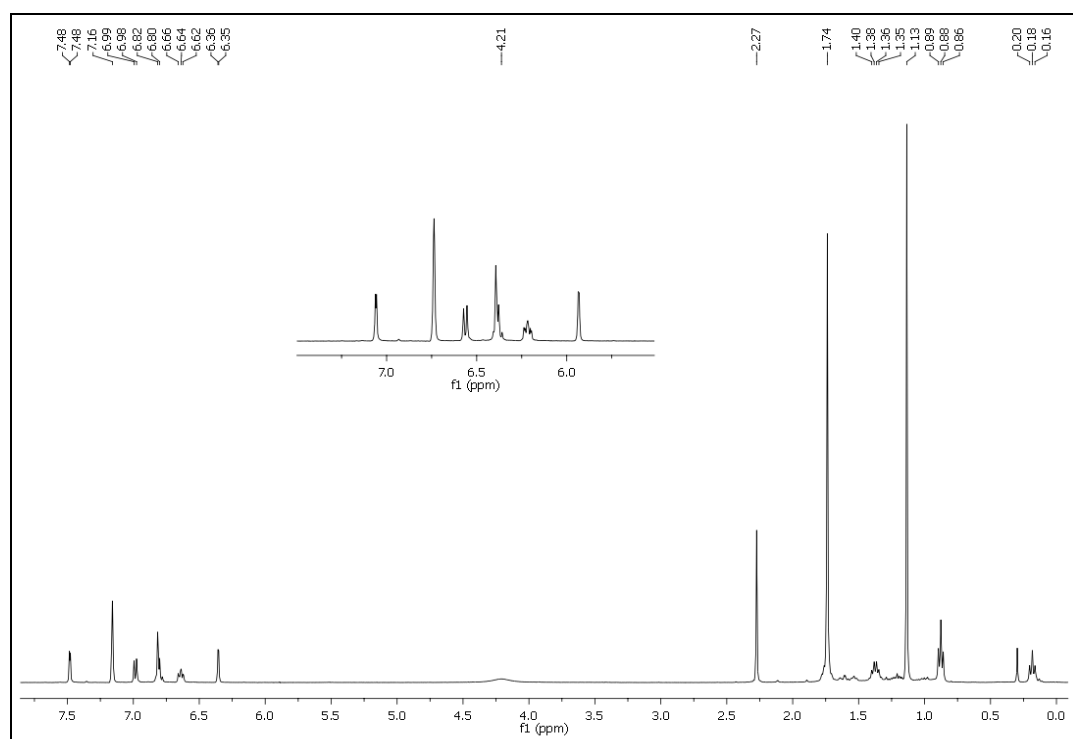


Figure S4. ^1H NMR of complex **4** (400 MHz, C_6D_6 , 298 K).

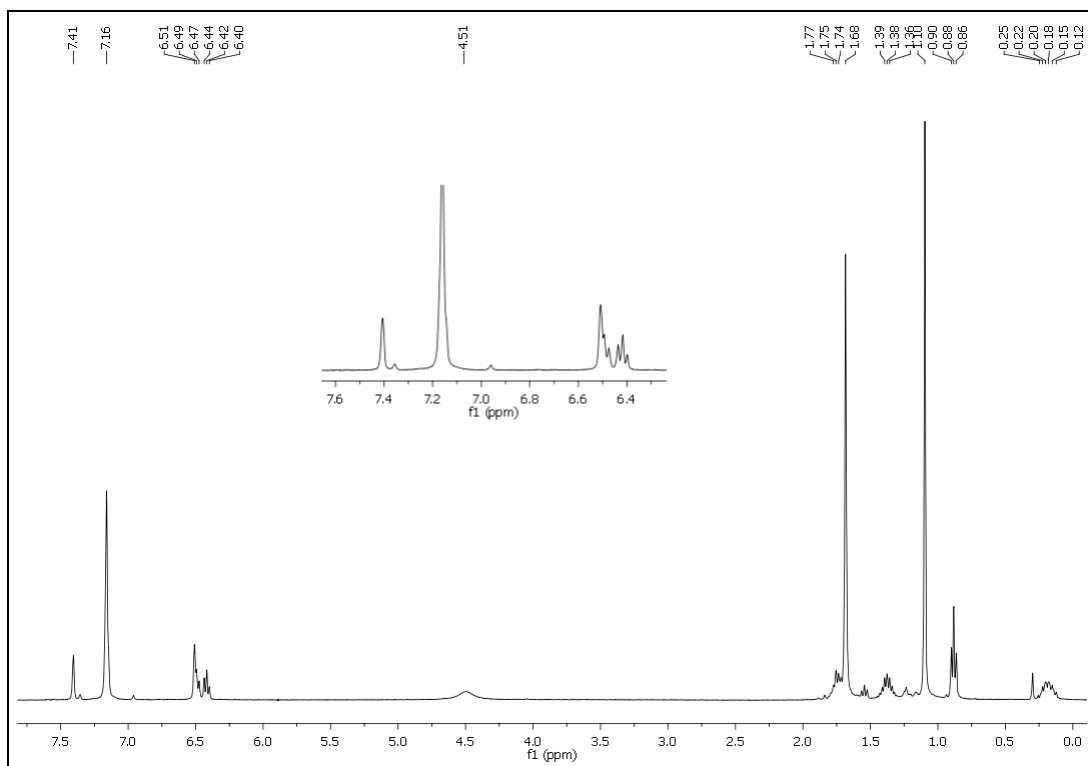


Figure S5. ^1H NMR of complex 5 (300 MHz, C_6D_6 , 298 K).

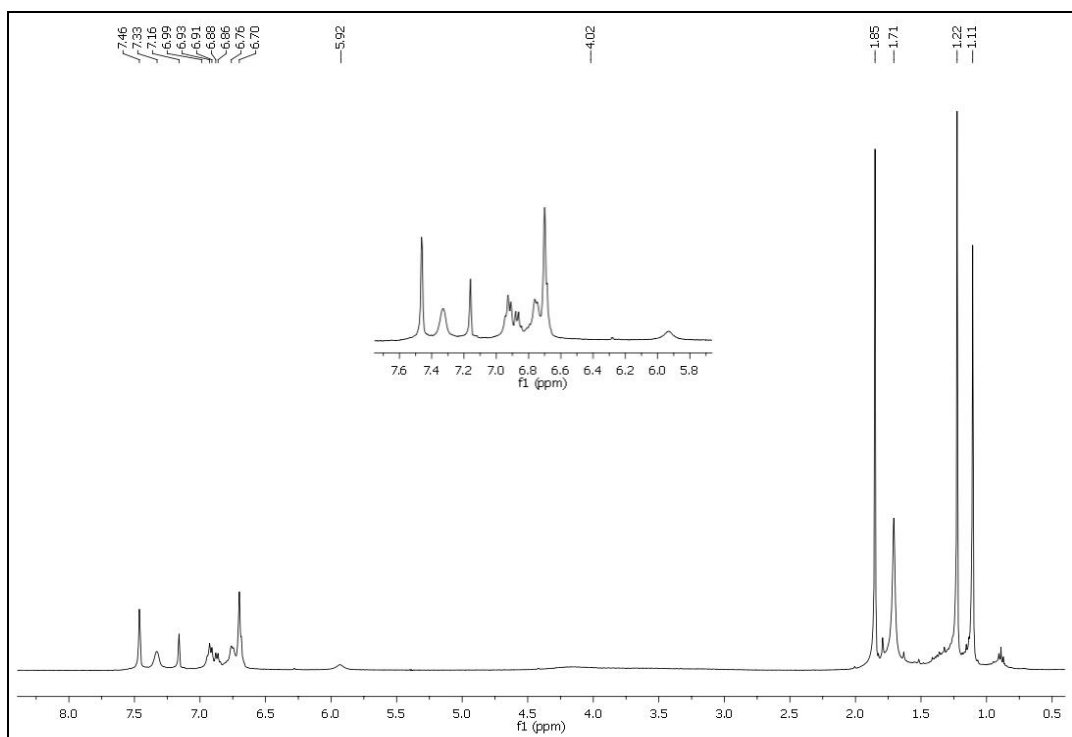


Figure S6. ^1H NMR of complex 6 (400 MHz, C_6D_6 , 298 K).

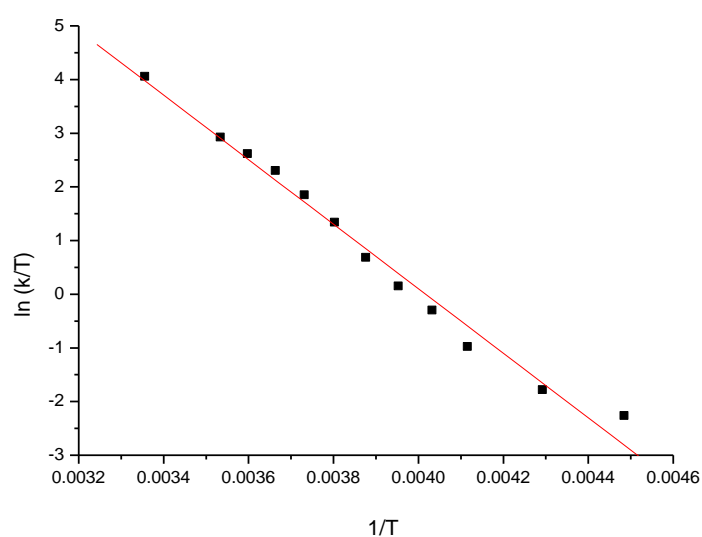


Figure S7 Eyring plot for the temperature-dependent fluxional process for complex **2**.

$$A = 24.152 \text{ (0.918)}$$

$$B = -6012.531 \text{ (236.540)}$$

$$R = -0.989 \text{ SD} = 0.2555$$

$$\Delta H^\# = 11.95 \pm 0.47 \text{ kcal mol}^{-1}$$

$$\Delta S^\# = 0.78 \pm 1.82 \text{ cal mol}^{-1} \text{ K}^{-1}$$

$$\Delta G^\# = 11.72 \pm 0.07 \text{ kcal mol}^{-1}$$

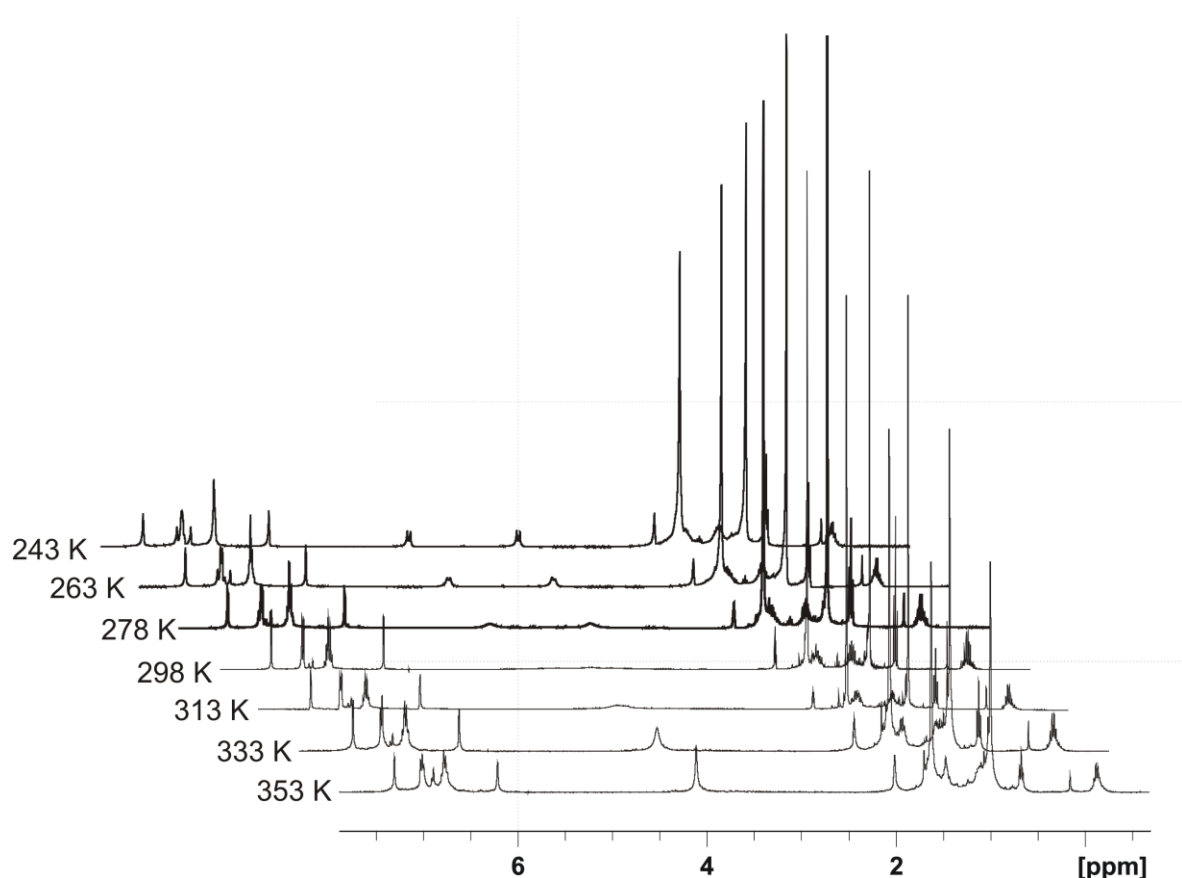


Figure S8. Variable-temperature ¹H NMR spectra of **3** in toluene-*d*₈.

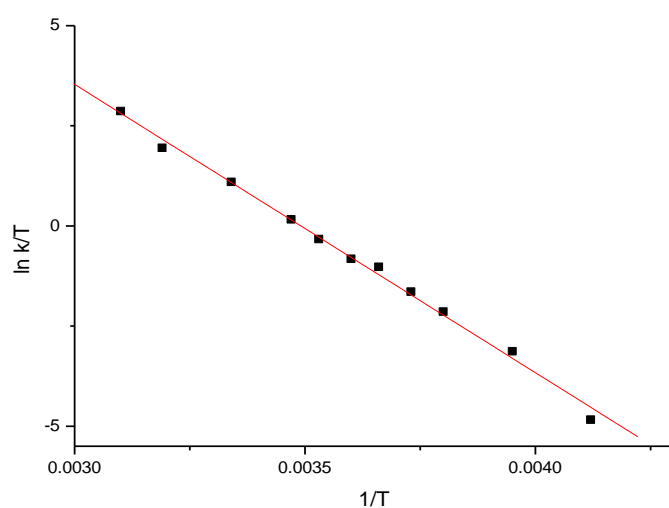


Figure S9. Eyring plot for the temperature-dependent fluxional process for complex **3**.

A = 25.14025 (0.59292)
B = -7201.26068 (164.60229)
R = -0.99766 SD = 0.16126
 $\Delta H^\ddagger = 13.49 \pm 0.07 \text{ kcal mol}^{-1}$
 $\Delta S^\ddagger = 2.74 \pm 1.18 \text{ cal mol}^{-1} \text{ K}^{-1} \text{ cal/mol K}$
 $\Delta G^\ddagger = 14.31 \pm 0.33 \text{ kcal mol}^{-1}$

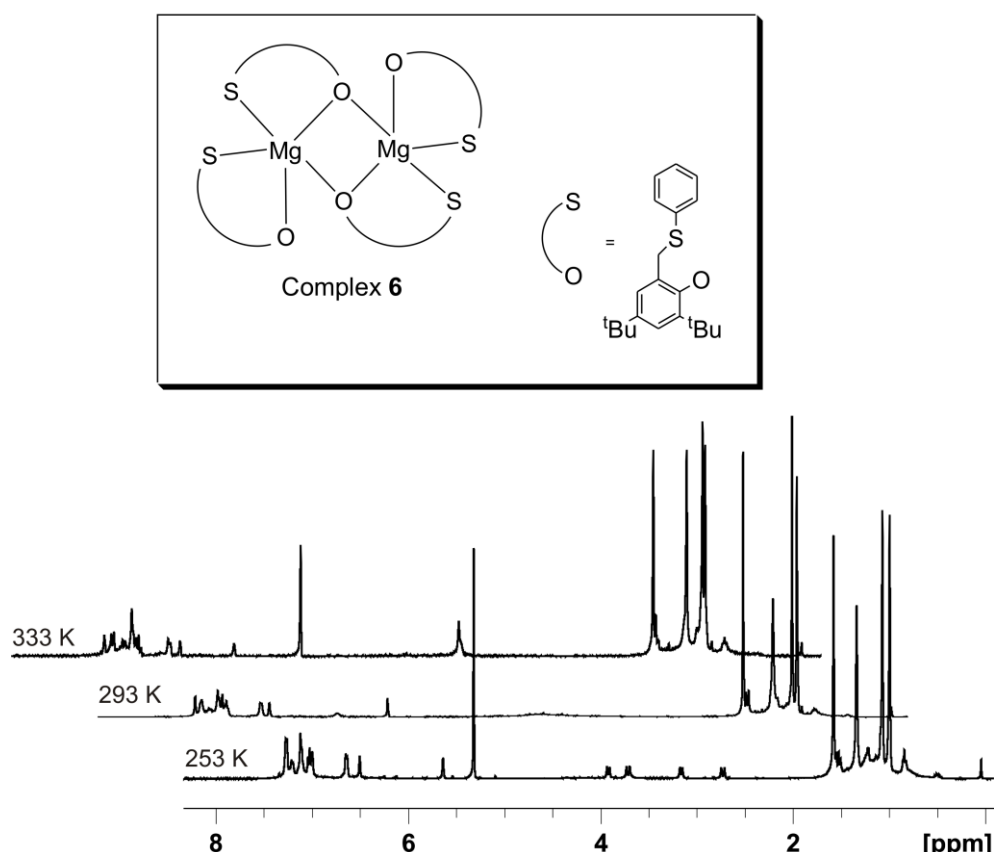


Figure S10. Variable-temperature ¹H NMR spectra of homoleptic complex **6** in CD₂Cl₂.

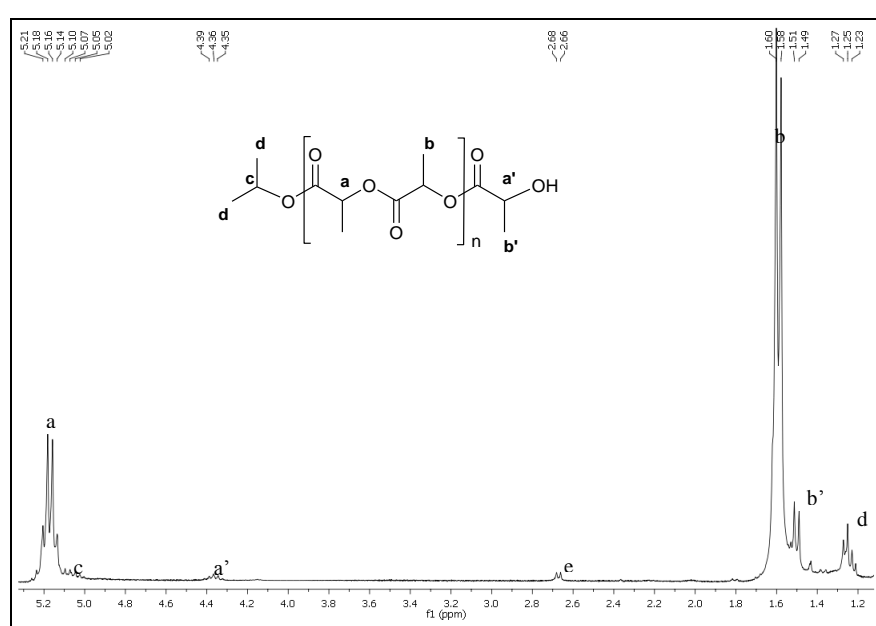


Figure S11. ¹H NMR spectrum (400 MHz, CDCl₃, 298 K) of oligomers of L-lactide obtained using [L-LA]₀/[**3**]₀ = 20, T= 25°C, t=5h.

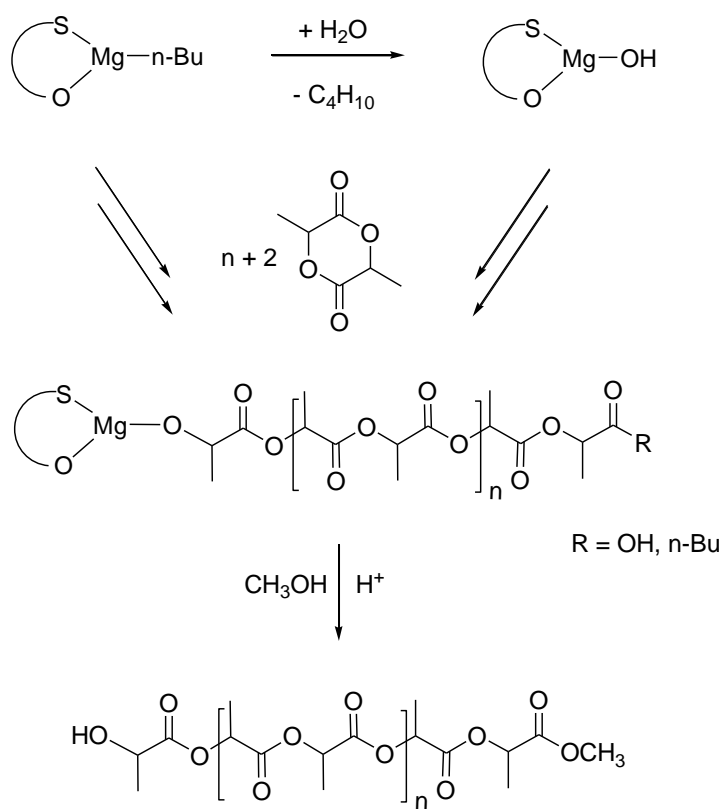


Figure S12. Plausible mechanism for the polymerization of L-LA by **3** in the absence of alcohol.

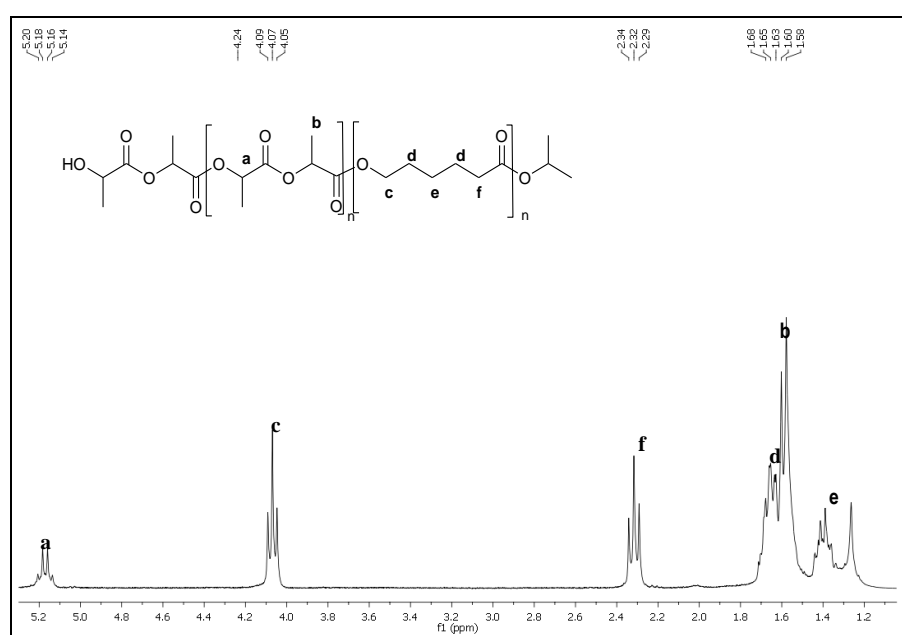


Figure S13. ^1H NMR spectrum of the CL-LA block copolymer

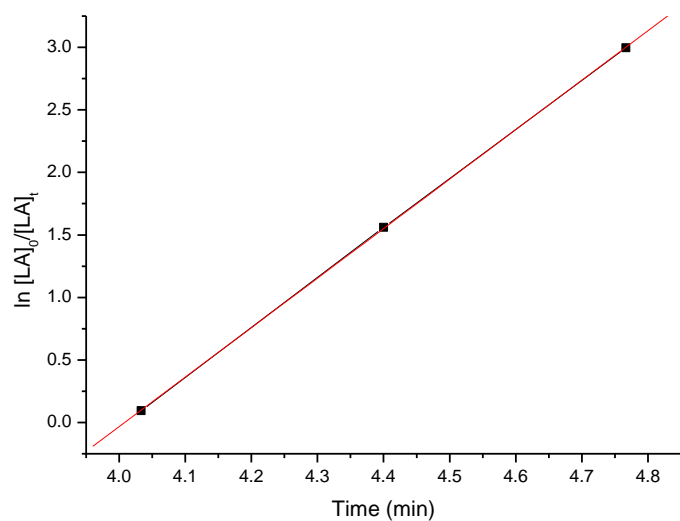


Figure S14. Enlargement of the linear part of graphic in Figure 6 in the MS. Pseudofirst-order rate constant is $k_{app} = 3.96 \pm 0.02 \text{ min}^{-1}$ ($R = 0.9998$) ($[3] = 9.1 \text{ mM}$; $[LA]/[3]/[\text{iPrOH}] = 100:1:1$; toluene-d₈ as solvent; $T = 343 \text{ K}$)

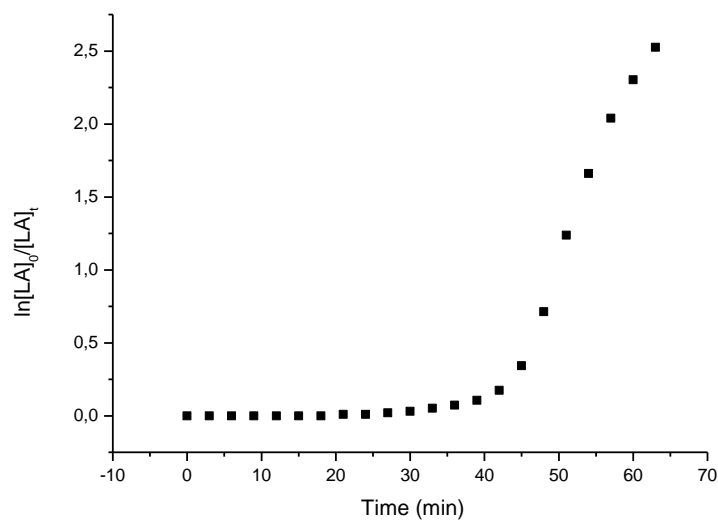


Figure S15. Semilogarithmic plot of LA conversion with time in toluene-d₈ at 323 K using **3** as initiator ($[3] = 9.1 \text{ mM}$; $[LA]/[3]/[\text{iPrOH}] = 50:1:1$)

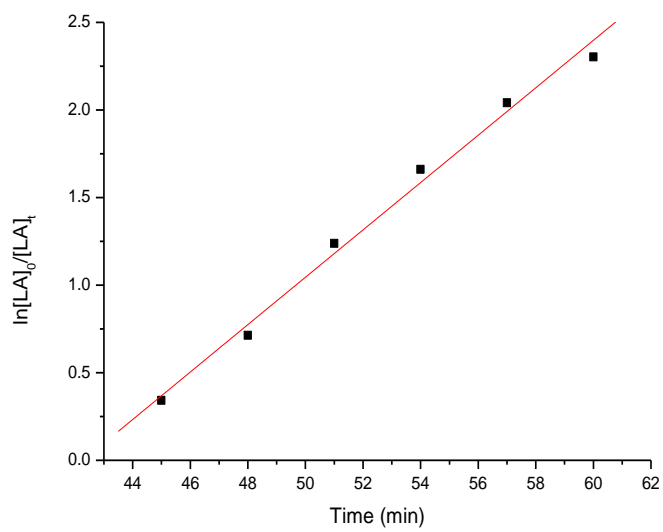


Figure S16. Enlargement of the linear part of graphic in Figure S14. Pseudofirst-order rate costant is $k_{app} = 1.35 \pm 0.06 \times 10^{-1} \text{ min}^{-1}$ ($R = 0.996$) ([**3**]=9.1 mM; [LA]/[**3**]/[iPrOH] = 50:1:1; toluene-d₈ as solvent; T = 323 K)